



Technological University Dublin
ARROW@TU Dublin

Articles

School of Food Science and Environmental
Health

2012-10

Hyperspectral Imaging for Non-Contact Analysis of Forensic Traces

Patrick Cullen

Technological University Dublin, pjcullen@tudublin.ie

G. Edelman

Academic Medical Center, Amsterdam, The Netherlands

T. Van Leeuwen

Academic Medical Center, Amsterdam, The Netherlands

M. Aalders

Academic Medical Center, Amsterdam, The Netherlands

E. Gaston

Innovació i Recerca Industrial i Sostenible, Castelldefels (Barcelona), Spain

Follow this and additional works at: <https://arrow.tudublin.ie/schfsehart>

 Part of the [Food Science Commons](#)

Recommended Citation

Cullen, P., Edelman, G. J., Van Leeuwen, T. G., Aalders, M. C., Gaston, E. Hyperspectral Imaging for Non-Contact Analysis of Forensic Traces. *Forensic Science International*, 22nd. October, 2012. doi:10.1016/j.forsciint.2012.09.012

This Article is brought to you for free and open access by the School of Food Science and Environmental Health at ARROW@TU Dublin. It has been accepted for inclusion in Articles by an authorized administrator of ARROW@TU Dublin. For more information, please contact yvonne.desmond@tudublin.ie, arrow.admin@tudublin.ie, brian.widdis@tudublin.ie.



This work is licensed under a [Creative Commons Attribution-NonCommercial-Share Alike 3.0 License](#)



Hyperspectral imaging for non-contact analysis of forensic traces

- [G.J. Edelman^a](#), , , ,
- [E. Gaston^b](#),
- [T.G. van Leeuwen^a](#),
- [P.J. Cullen^c](#),
- [M.C.G. Aalders^a](#)

- ^a Department of Biomedical Engineering and Physics, Academic Medical Center Amsterdam, The Netherlands
- ^b Innovació i Recerca Industrial i Sostenible, Castelldefels (Barcelona), Spain
- ^c School of Food Science and Environmental Health, Dublin Institute of Technology, Ireland

Abstract

Hyperspectral imaging (HSI) integrates conventional imaging and spectroscopy, to obtain both spatial and spectral information from a specimen. This technique enables investigators to analyze the chemical composition of traces and simultaneously visualize their spatial distribution. HSI offers significant potential for the detection, visualization, identification and age estimation of forensic traces. The rapid, non-destructive and non-contact features of HSI mark its suitability as an analytical tool for forensic science. This paper provides an overview of the principles, instrumentation and analytical techniques involved in hyperspectral imaging. We describe recent advances in HSI technology motivating forensic science applications, e.g. the development of portable and fast image acquisition systems. Reported forensic science applications are reviewed. Challenges are addressed, such as the analysis of traces on backgrounds encountered in casework, concluded by a summary of possible future applications.

Keywords

Forensic science, Hyperspectral imaging, Chemical imaging, Spectroscopic imaging, Detection, Identification, Aging

Introduction

The detection and identification of forensic traces are crucial in crime scene investigations. For this purpose a wide range of techniques is available, including chemical enhancement techniques and the use of light sources with 15 to 30 nm bandwidths, which increase the contrast between a trace and its background. Many of these techniques are, however, either destructive or subject to human interpretation. Hyperspectral imaging (HSI) is suitable for the non-contact identification of evidence, thus minimizing the risk of contamination and destruction of traces. HSI integrates conventional imaging and spectroscopy to obtain a three dimensional data set containing both spatial and spectral information of a specimen. In addition, analysis of the temporal behavior of spectra can give insight in the chemical changes within the specimen, which can be used for age estimation purposes. Estimation of the age of forensic traces provides investigators with valuable information, which can assist the reconstruction of the timeline of events.

HSI was originally developed for remote sensing applications utilizing satellite imaging data of the earth [1] but has since found application in such diverse fields as food science [2], pharmaceuticals [3] and medical diagnostics [4]. Hyperspectral images are analogous to a stack of images, each acquired at a narrow spectral band. Like spectroscopy, HSI can be applied in different parts of the electromagnetic spectrum, e.g. ultraviolet (UV), visible (Vis), near infrared (NIR), mid infrared (IR) or even the thermal infrared range. In these regions reflectance, transmission, photoluminescence, luminescence or Raman scattering can be recorded by hyperspectral cameras with a spectral resolution similar to miniature spectrographs. Spatial resolutions can be adapted to the application, which range from microscopic to landscapes. Advantages of HSI include speed of data acquisition, reduction of human error, no destruction of traces, no specimen preparation, and the ability to illustrate the results.

HSI is a powerful emerging tool for the analysis of forensic traces. Latent traces can be detected and visualized by using spectral differences to obtain optimal contrast between a trace and its background. Individual spectra give information about the chemical composition of the specimen,

which is useful for identification and quantification purposes, and the spatial distribution of traces is simultaneously recorded. In the last decade, HSI has proven to be a valuable technique for the imaging of latent fingerprints and the detection of trace materials within these prints. HSI is also emerging in other fields of forensic science and has shown its value in comparative research of materials including fibers, paint chips, or inks, where the question arises whether two traces share common origin. The possibility of viewing spectral and spatial information side by side is advantageous in these cases.

Recent developments in HSI technology offer added potential for forensic science investigations. Because HSI systems are becoming increasingly portable, they may be used at the scene of investigation, where traces can be viewed and interpreted in the original context. The development of fast scanning systems enables investigators to scan a complete scene, which reduces the workload in forensic laboratories and quickly provides investigators with valuable information which can lead the investigation.

This paper gives an overview of the principles, instrumentation and analytical techniques involved in HSI, followed by a review of recent forensic science applications. We limited our scope to HSI applications using reflectance, photoluminescence, transmission or Raman scattering. Because forensic traces are typically encountered in many different environmental circumstances, their analysis brings specific challenges, which are also addressed. To conclude, possible future applications are summarized.

Hyperspectral imaging

Interaction of light and matter

The interaction between light and a specimen is determined by the optical properties of the specimen and the incident light. As hyperspectral imaging measures such interaction, it may be used to characterize the material. In practice this involves illumination of the object under investigation.

Commonly, the first interaction will be on the specimen surface where part of the light will be reflected (Figure 1a). This part contains no to little information from within the medium but is governed by the index of refraction difference between media. Upon entering the material, the light can be scattered or absorbed.

Scattering is the process by which light interacts with structures in a specimen and causes a change in direction of propagation, depending on the wavelength, size of the particle and index of refraction differences (Figure 1b). The majority of light is scattered at the identical wavelength of the incident light, a process referred to as elastic scattering. There may also be a small fraction that will be inelastically scattered (Raman scattering) which will cause wavelength shifts corresponding to the vibrational states of the molecules in the specimen (Figure 1c). Raman scattering can be measured to chemically analyze the scattering specimen.

The absorption properties of a chemical compound are wavelength dependent. Absorption in the visible wavelength range corresponds to the electronic states of the molecule, while absorption in the NIR and IR is determined by the vibrational modes. Upon relaxation, return to the ground state, the energy will be released in the form of radiation (heat or photoluminescence) or by transfer to another molecule. So both the spectral absorption and, if present, the induced photoluminescence can be measured to identify the chemical contents of a specimen using hyperspectral cameras in reflectance, or transmission mode (Figure 1d/e). Quantitative analysis, however, is complicated because the length of the path travelled by the detected light depends on the optical properties of the specimen [5].

Hyperspectral formation

Hyperspectral images are analogous to a stack of images, each acquired at a narrow spectral band. The resulting data set is a three-dimensional block of data, the so-called hypercube, with two spatial (x,y) dimensions and one wavelength (λ) dimension (Figure 2). This hypercube provides images for each wavelength (λ_i) and a spectrum can be obtained from each individual pixel (x_i, y_k), as depicted in Figure 2.

Obtaining information in all three dimensions of a hypercube simultaneously is currently not feasible; instruments can only capture two dimensions at a time. Temporal scanning is needed to create a three-dimensional hypercube by stacking the two-dimensional data in sequence. There are three ways of acquiring a hypercube (Figure 3), commonly known as point scanning (or whiskbroom), line scanning (or pushbroom), and area scanning (or staredown). These descriptive names refer to the hardware methodology used to acquire the hypercubes:

- In a point scanning system, a complete spectrum is acquired at a single point. Light originating from this point enters the objective lens and is separated into different wavelengths by a spectrometer and detected by a linear array detector. Once spectral acquisition is completed, the spectrum of another point can be recorded. Scanning has to be performed in both spatial directions to complete the hypercube.
- In the case of line scanning systems, the spectra of all pixels contained in one image line are acquired simultaneously. The light is dispersed onto a two dimensional charge coupled device (CCD) detector. This way, a two dimensional data matrix with the spectral dimension and one spatial dimension is acquired. The second spatial dimension of the hypercube is achieved by scanning across the specimen surface in a direction perpendicular to the imaging line. This means that relative movement between the object and detector is necessary, which may be achieved either by moving the specimen (e.g. using a translation stage or a conveyor belt) and keeping the hyperspectral camera in a fixed position or by moving the camera and keeping the specimen fixed.
- An area scanning system also acquires a two-dimensional data matrix but in this case the data represent a more conventional image with two spatial axes. A complete hypercube is obtained by collecting a sequence of these images for one wavelength band at a time. The wavelength of incoming light in this configuration is typically modulated using a tunable filter.

System optimisation for forensic science applications

Typical hyperspectral imaging systems contain the following components: objective lens, wavelength modulator, detector, illumination, and acquisition system (Figure 4). All these components can be

adjusted to the requirements of the application. The forensic environment of analysis may range from laboratory to field conditions, whereas the areas of interest may range from the microscopic to landscapes. As for conventional imaging, different objective lenses can be chosen to obtain the right spatial resolution for each application, e.g. macroscopic lenses, zoom lenses, wide angle lenses etc. For analysis on a microscopic scale, the HSI system can be coupled to a microscope.

Acousto-Optic Tunable Filters (AOTFs) [6] and Liquid Crystal Tunable Filters (LCTFs) [7] are the two most common wavelength modulators employed. Major drawbacks of these filters are their size and costs. Recently, HSI systems have been developed and commercialised using Fabry-Pérot filters (Innopharmalabs, Ireland). Another recent innovation employs the use of a tunable laser system based on Optical Parametric Oscillator (OPO) technology [8]¹¹¹¹¹¹¹¹¹¹¹¹¹¹¹¹¹¹¹¹¹¹¹¹¹¹¹¹¹¹¹¹¹¹¹¹¹¹, which replaces the broadband light source, thus removing the need for a wavelength modulator. The benefits of Fabry-Pérot filters and tunable lasers compared to tunable filters are their small size and weight, speed of wavelength tuning and high optical throughput. The development of these new technologies offers potential for low cost, hand held, portable HSI with the desired resolution for trace analysis in forensic science applications.

After the light is separated into different wavelengths the detector, e.g. a charge coupled device (CCD), measures the intensity of the collected light. The pixels in the CCD sensor can be arranged in one-dimensional or two-dimensional arrays, resulting in line detectors and area detectors [9]. Detectors for the mid-infrared region are also available, such as lead selenide (PbSe), indium antimonide (InSb), and mercury cadmium telluride (MCT). To ensure sensitivity of the detector to low light intensities in the infrared regions, the detector may have to be cooled. The CMOS image sensor is another detector that has the potential to compete with CCD. Typical advantages as high speed, low cost, low power consumption, and small size for system integration make them prevail in the consumer electronics market (e.g. low-end camcorders and cell phones). However, the dynamic range and the sensitivity are lower than those of CCD detectors [9].

The choice of the light properties (broadband vs monochromatic, specular vs diffuse, etc.) and consequently the illumination source (halogen, LED, laser, etc.) and lighting arrangement are crucial for the performance and reliability of the system. Halogen lamps, commercially available in various forms, are most common broadband illumination sources used in hyperspectral applications. Halogen lamps can be used directly to illuminate the target (like room lighting) or can be delivered through an optical fiber. Light emitting diode (LED) technology has advanced rapidly during the past few years, and both narrowband and broadband light generators are currently available in the market. This technology is a relatively inexpensive, robust and reliable alternative to halogen lighting, and its use for hyperspectral imaging is likely to expand in the near future, with particular benefits for portable systems. Unlike broadband illumination sources, lasers are powerful directional monochromatic light sources, which make them interesting candidates for photoluminescence and Raman applications. The use of aforementioned tunable light sources is still limited in hyperspectral imaging applications but they offer promising scope for specific applications including trace analysis. The implementation of digital micro-mirror devices (DMDs) is another recent development in HSI [10]. In this setup, only the region of interest is illuminated. Such systems reduce variations in the spectra arising from scattered light from the background and nearby objects.

Finally, the image acquisition system can be optimized for the application. The desire for on-line monitoring within the process industries has seen the emergence of real-time online systems typically employing line-scanning approaches. This line scanning setup also offers potential for large-scale forensic science applications, where instead of using a moving stage or conveyor to pass a specimen or product past the detector, the detector itself is moved over a large stationary area of interest such as a wall, a floor or an entire scene of investigation (see Figure 5).

Data analysis

Upon detection, analysis of the data provided in the hypercube is required. Grahn and Geladi detail the types of treatment that can be applied [11]. A summary of processing steps is given below.

Calibration

The raw data in a hypercube not only result from the chemical composition of a specimen, but also from the illumination intensity, the sensitivity of the detector and the transmission of the optics [12]. The influence of these factors is a function of wavelength, but may also show spatial variations. Spectral and spatial calibration is required to compensate for this. Calibration measurements typically performed for reflectance measurements consist of acquisition of the dark response of the system, measured while covering the lens and dimming the light source, and the response of a uniform, high reflectance reference. Using these data, the reflectance (R) can be calculated as follows:

$$R = (I_{\text{specimen}} - I_{\text{dark}}) / (I_{\text{reference}} - I_{\text{dark}}),$$

where I_{specimen} is the intensity of the reflectance measurement of the specimen, I_{dark} the intensity of the dark response, and $I_{\text{reference}}$ the intensity of the uniform reference.

It is considered good practice to carry out calibration on a daily basis, as small changes in electrical power sources, illumination, detector response and system alignment may result in changes in the detected response. Inclusion of internal reference standards in each hyperspectral image acquired is also recommended, which allows monitoring the performance of the system over time.

Spectral pre-processing

Spectral information can be used to gain knowledge about the chemical composition of a specimen. However, several non-chemical origins cause systematic variations between spectra, unrelated to the chemical composition of a specimen, including specular reflections, scattering effects due to surface inhomogeneities, varying object – illumination distances and random noise. A number of spectral pre-processing techniques can be applied to reduce these variations, e.g. smoothing, offset correction, normalization, mean centering, standard normal variate (SNV) correction [13], multiplicative scatter correction (MSC) [14], and Savitzky-Golay differentiation [15]. The effect of MSC and differentiation is demonstrated in Figure 6; MSC removes variation resulting from scattering

effects, first and second order differentiation eliminate a constant offset or linear baseline, respectively, and can be used to resolve overlapping peaks originally appearing as shoulders.

Spectral analysis

Spectral data analysis attempts to address what different components are present in the hypercube, in which concentration and how they are distributed. In some cases the intensity at a single wavelength, the integrated intensity (area) under a spectral peak, or ratios of intensities at different wavelengths can be sufficient for the analysis. However, using these methods, the large amount of spectral information available is not completely exploited. To reduce the amount of variables, while keeping the maximum of variation in the data, Principal Component Analysis (PCA) can be applied, which is a popular multivariate chemometric method.

In general, spectra are compared to other spectra in the hypercube or to reference spectra from an external library using a similarity measure, e.g. the Euclidean distance, Pearson's correlation coefficient or the spectral angle [16]. Spectral unmixing can be applied to decompose a measured spectrum into a collection of constituent spectra [17-19]. Clustering and classification techniques use the spectral information contained in the hypercube and identify regions with similar spectral characteristics. Clustering techniques are unsupervised methods, e.g. k-nearest neighbors [20], which require no a priori information about the dataset to achieve clustering. Supervised classification methods, including partial least squares discriminant analysis [21], and spectral angle mapping [22], require the selection of well-defined and representative calibration and training sets for classifier optimization. On the other hand, hyperspectral image regression enables the prediction of constituent concentrations at the pixel level, thus enabling their spatial distribution in a specimen to be visualized. Numerous approaches are available for the development of regression models (e.g. partial least squares regression, principal components regression [14]) .

Image processing

Image processing is performed to convert the contrast developed by the previous steps into a picture showing the component distribution. Additionally, a single wavelength image can be selected showing the highest contrast between different components. Grayscale or color mapping with intensity scaling is frequently used to display compositional contrast between pixels in an image. False color mapping, in which two or more images at different wavebands are combined to form a new color image may be employed to enhance apparent contrast between distinct regions of a specimen.

An interesting other approach for presenting the results was demonstrated by Alsberg et al [23], who projected the results of HSI analysis back onto the scene to highlight chemical differences otherwise invisible to the naked eye. This non-destructive technique provides information similarly to traditional forensic methods, e.g. the use of luminol to highlight blood stains at a scene of investigation, and can be useful to guide investigators in their search for traces.

Forensic science applications

Although hyperspectral imaging has mainly been used for the analysis of fingermarks, studies are also reported on several other forensic traces, including drugs, hair, dentin, bruises, blood stains, condoms, inks, tapes, firearm propellants, paints and fibers. These applications are summarized in Table 1 and described in more detail below.

Fingermarks

Latent fingermarks are a complex mixture of eccrine deposits from the finger and sebaceous deposits resulting from touching other body parts, such as the face [24]. Eccrine deposits mainly consist of amino acids, inorganic compounds, and proteins, while sebaceous material consists primarily of fatty acid esters [25]. The chemistry of these residues varies among individuals and it shows increasing

amounts of sebaceous deposits with age [26,27]. Fingerprint detection techniques aim to create contrast between the ridge details of a latent fingerprint and the background on which it is located.

Detection and enhancement of untreated fingerprints

Several authors recently evaluated the possibility of detecting untreated latent fingerprints using HSI. Exline et al used visible reflectance and photoluminescence HSI to detect untreated latent fingerprints on plastic and paper [28]. Resulting images were compared to images created with a conventional forensic imaging system, in which different excitation and observation wavelengths could be chosen. While both methods succeeded in visualizing latent fingerprints on plastic, HSI showed enhanced contrast on paper surfaces. Processing tools used included background division, offset correction, normalization and PCA. In a further study Payne et al optimized this visualization technique by using different processing tools to achieve an improved image [29].

Unlike visible HSI, NIR and IR HSI yield information about the vibrational modes of a molecule, and thus give additional information about the chemical composition of the material being studied. Bartick et al were the first to show the application of NIR and IR HSI for imaging latent fingerprints, using spectral bands indicative of the chemical components of the deposited material [26]. They successfully visualized fingerprints deposited on aluminum coated microscope slides.

Crane et al demonstrated the ability of IR HSI to detect latent untreated fingerprints on various porous backgrounds (copier paper, cigarette butt paper, U.S. dollar bill, postcard) and non-porous backgrounds (trash bags, a soda can, tape) [27]. Fingerprints on the soda can and a black trash bag were clearly visible when viewing the intensity band image at 9842 nm (asymmetric O-C-C stretch ester) (see Figure 7). On other backgrounds, more complicated processing tools were required, like PCA, and second derivatives. Processing with these tools rendered most prints clearly visible, even on paper-based porous surfaces. However, the position of the fingerprints was known before collecting the images.

In two papers, Tahtouh et al also described the application of infrared HSI to the visualization of untreated fingerprints ^{2,3}. Results indicated that the infrared spectra of many untreated

fingermarks show peaks due to C-H stretching vibrations around 3333 nm, mainly due to fatty acid residues. These peaks are common to most organic compounds, but they can be used to visualize fingermarks against some backgrounds, like metals, minerals, and ceramics, that do not contain C-H bonds. For fingermarks on other backgrounds, they stated that some type of chemical enhancement technique is required prior to hyperspectral imaging.

Bhargava et al described an approach to use IR HSI to reveal latent fingermarks overlaid on top of one another, each made under different hand washing conditions [32]. Differences observed in the absorbance of the C-H stretching mode and other vibrational modes in the spectra indicated that the two prints had different chemical compositions. Because of this variation, linear unmixing applied to the spectral content of the data could be used to provide images revealing both superimposed fingermarks.

Detection and enhancement of treated fingermarks

Conventionally, fingermarks are treated with chemicals to increase sensitivity and/or contrast with the background. On porous surfaces such as paper, ninhydrin and DFO (1,8-diaza-9-fluorenone) are often applied, which both react with amino acids present in fingerprint ridges, causing a purple color or photoluminescence respectively [33]. On non-porous surfaces such as glass and plastic, cyanoacrylate (superglue) is the most widely used method [33]. Cyanoacrylate fumes polymerize in the presence of moisture and greasy component of the fingerprint. The contrast of fingerprints treated with cyanoacrylate can be further enhanced by various methods including luminescent staining [28].

Exline et al [28] and Payne et al [29] investigated the potential of HSI to increase the contrast and visual quality of treated fingerprints compared to traditional methods of detection. Using visible HSI they investigated fingerprints treated with ninhydrin, DFO, cyanoacrylate, and fluorescent dyes. In some cases, HSI showed significant enhancement over the traditional method, which was mainly due to the suppression of a highly fluorescent background or isolation of the developed latent

impression. Hence, the minutiae details were visible using HSI where they were not with the traditional method. Such examples were examined and compared to the original donor's prints by a certified fingerprint examiner. This process verified that the enhanced detail coincides with actual naturally occurring detail. The added information brought by HSI could sometimes be sufficient for exclusion purposes, whereas the traditional examination would lead to an inconclusive result. In a similar study Miskelly and Wagner used HSI to image chemically treated fingerprints deposited on a newsprint and an aluminum soda can [34]. They showed that background correction is an important step in the visualization of fingerprints on difficult backgrounds.

Although visible HSI is an improvement compared to traditional techniques, it is not always possible to obtain acceptable fingerprint images, for example when the background is highly fluorescent, colored or patterned. However, most dyes that absorb or fluoresce strongly in the visible region are reflective in the NIR [35]. This means that background interferences from dyed surfaces should be reduced when working in the NIR, compared to visible imaging. Maynard et al systematically imaged latent fingerprints on porous, non-porous and semi-porous surfaces [35]. Next to a wide variety of conventional chemical and physical treatments, NIR laser dyes were tested for their ability to produce NIR photoluminescence. Both absorption and photoluminescence properties of the treated marks were examined using NIR HSI. The most suitable enhancement techniques depend on the type of surface. Fingerprints on colored, printed or watermarked surfaces were imaged in the NIR region without interference from the background color, both in absorbance and in photoluminescence modes. In these cases, imaging in the NIR region provided advantages over imaging in the visible region.

Background interference problems in the visible region can also be solved by showing differences in chemical composition of the print and the background using mid-infrared HSI, as shown by Tahtouh et al ^{2,3}. Infrared HSI of chemically treated fingerprints was carried out on several challenging backgrounds. It was found that infrared HSI gives high quality images of cyanoacrylate-fumed fingerprints on polymer banknotes and aluminum drink cans, regardless of the printed

background. Attempts to acquire images of fingerprints on paper-based porous surfaces treated with established reagents such as ninhydrin were all unsuccessful due to the swamping effect of the cellulose constituents of the paper.

In addition to the chemicals commonly used to create contrast between fingerprints and backgrounds, Tahtouh et al tested four novel chemicals which can be visualized with IR HSI [36]. These were chosen for their potential to produce a strong, isolated infrared spectral band. Each chemical polymerized selectively on fingerprint ridges and high quality images were obtained of fingerprints on difficult backgrounds.

Detection and identification of trace contaminations in fingerprints

Next to eccrine and sebaceous deposits, fingerprints may be contaminated by exogenous substances of various sources. These substances might include drugs of abuse, traces of explosives or gunshot residue. Traces found at the scene of investigation can be directly related to an individual by its presence in the fingerprint. Many of the approaches involved in collecting traces are destructive. For example, swabbing objects destroys fingerprint deposits within the area. Because of its non-destructiveness, hyperspectral imaging can be used to simultaneously image a latent fingerprint and detect trace information contaminating it.

In 2005, Grant et al had volunteers handle a mixture of common materials before giving fingerprints [37]. When looking at the fingerprints under a visual light microscope, it was impossible to distinguish particles from different materials. However, by using infrared HSI, vibrational spectra of individual particles were obtained and identified by comparison with a spectral library.

In a similar study, Bhargava et al examined traces of explosives within a latent print, using an infrared HSI system [32] (Figure 8). They used spectral subtraction to eliminate the effects of latent material on traces. Unique spectral features of the traces were used to provide images of the distribution of these traces. From pixels dominated by the material the full spectrum of the traces was obtained and compared to databases for identification.

Ng et al tested different spectral searching algorithms for their efficacy in finding targeted substances deposited within fingerprints [24]. Out of a range of algorithms which included conventional Euclidean distance searching, the spectral angle mapper and correlation algorithms gave the best results when used with second-derivative image and reference spectra. Aspirin, diazepam, caffeine, and explosive components were successfully detected and located in a fingerprint.

Emmons et al used Raman HSI to examine fingerprints contaminated with traces of explosives (532 nm excitation) [38]. To determine if explosives were present in the fingerprints measured, the resulting spectra of each pixel were compared to a spectral library of pure reference specimens of explosives. A false color picture was created which indicated the possible presence of explosives. Significant differences in the spectra could be used to differentiate between different types of explosives.

Chen et al applied IR HSI and principal component analysis to distinguish between overlapping fingerprints based on exogenous compounds [39]. After creating a blank fingerprint containing natural secretions, a second finger contaminated with an explosive solution was printed on top of it. Although trace residues of the explosives trapped between the fingerprint ridges could be clearly detected, it was not evident which fingerprint these chemicals belonged to in cases with overlapped prints.

All the above studies examined fingerprints left on surfaces, which are ideal for infrared reflection analysis. In a forensic science scenario, reflective substrates such as a doorknob, knife blade, or handle should be relatively straightforward for analysis similar to the laboratory situation [24]. However, surfaces such as glass, plastic, wood, paper, cloth, etc., will all have their own (sometimes strong) infrared absorptions. These IR absorptions of the underlying surface will mask some parts of the spectrum, rendering these regions unusable for spectral identifications. The effectiveness of finding foreign materials within latent fingerprints in these cases will be dependent on having enough identifying spectral features outside these spectral regions [37].

Other traces

Apart from the analysis of fingerprints, the benefits of HSI can be exploited for the analysis of many other traces of importance in forensic science. Latent traces can be detected and visualized by using spectral differences to obtain optimal contrast between a trace and its background. Individual spectra give information about the chemical composition of the specimen, which is useful for identification, quantification, or age estimation. The possibility of viewing spectral and spatial information side by side is an advantage in comparative research of e.g. fibers, paint chips, or inks, where the question arises whether two traces share common spectral features. Several applications described in literature are reviewed below.

Kalasinsky et al were the first to demonstrate the value of infrared HSI for determining drugs of abuse in hairs [40]. By examining only the interior portion of the hair, drugs exclusively resulting from human ingestion were measured and distinguished from drugs that made contact with the outside of the hair. After microtoming the hair, IR hyperspectral images were obtained of the cortex and the medulla. Drug free hairs of different sources all correlated with standard spectra of proteins. A hair of a chronic drug abuser of hydromorphone was analyzed similarly. Subtraction of the drug free reference spectra yielded a strong indicative band at 5824 nm, which was also present in reference hydromorphone spectra. An intensity band image at 5824 nm showed that the drug was concentrated in the center of the hair. This way, relative drug concentrations across the hair could be successfully determined and visualized. In a further study, Kalasinsky showed the distribution of drugs in human hairs, which is critical information to validate drug testing data [41]. IR HSI on hairs doped with 6-acetyl morphine (a metabolite of heroin) and cocaine, showed that hydrophobic drugs tend to bind to the medulla of the hair while hydrophilic drugs tend to be spread throughout the cortex of the hair.

Hair color is basically determined only by eumelanin and pheomelanin, whose varying ratios produce the observed color. In forensic science casework, hair color is normally classified through

visual comparison with standardized plates. Birngruber et al investigated the possibility to objectively distinguish hairs from different persons using hyperspectral imaging in the Vis-NIR range [42]. They demonstrated an extreme intra-individual variability in the spectra of single hairs from an individual. Because of this, hairs undistinguishable on the basis of morphology could not be distinguished based on the hyperspectral images.

The chemical composition of the dentinal part of the tooth evolves with increasing age. Tramini et al measured 30 human teeth with Raman HSI (with 632 nm laser excitation) and were able to identify a very small quantity of dental material coming from skeleton debris or biological remains, and determine which kind of tissue it was [43]. They created a PLS regression model to predict the age of an individual based on Raman spectra of his teeth. The model was tested on four teeth, and an age estimation was obtained with a mean error of 5 years.

The analysis of bruises, or aging of bruises in particular, can give important evidence in cases of domestic violence or child abuse. Several studies have been performed as initial steps towards the aging of bruises using HSI. A bruise is formed after blunt trauma, which results in blood being present in the skin. In time, hemoglobin in the blood is degraded into other products, including bilirubin. Both hemoglobin and bilirubin have typical spectral features in the visible region [44]. Payne et al showed the possibility to use HSI to differentiate pure blood from blood with bilirubin based on these spectral features [45]. Randeberg et al presented hyperspectral images of bruises on porcine and human skin [46]. They used minimum noise fraction transform, a statistical method similar to PCA, to classify the injuries. Stam et al described how HSI can be used to accurately determine the areas covered by hemoglobin and bilirubin in the bruise, by fitting pixel spectra with a combination of reference spectra of chromophores present in bruises [47].

Similarly, reflectance spectra of blood stains can be spectrally unmixed to derive the relative amounts of oxyhemoglobin, methemoglobin and hemichrome within the blood stains, as demonstrated by Edelman et al [17,18]. By comparison of spectra derived from hyperspectral imaging data with a non-linear least squares fit of the theoretical spectra of the hemoglobin

derivatives, blood stains were identified in a simulated crime scene and could be distinguished from similarly colored substances [17]. Additionally, the temporal behavior of the amount of hemoglobin derivatives provided insight in the chemical changes occurring in time, and could be used to estimate the age of blood stains [18]. Figure 9 shows a simulated crime scene in which fresh and older blood stains were distinguished using this method.

Important evidence pertaining to sexual assault cases can be provided by the identification of condom lubricant components. In an exploratory study, Wolfe and Exline showed that some of the most common materials found in condom lubricants can be accurately characterized by Raman HSI (with 532 nm laser excitation) without the extensive specimen preparation inherent to other analytical methods [48]. Using the CH stretching region of the Raman spectrum, they were able to generate contrast based on spectral differences.

To demonstrate the potential of HSI in forensic investigations, Payne et al compared HSI to point measurements performed with traditional spectrometers [49]. They used Vis/NIR HSI to differentiate between a set of tapes and adhesives, a set of inks (Figure 10) and two brands of firearm propellants, based on reflectance and photoluminescence properties. They conclude that HSI offers significant advantages, mainly because a large number of specimens can be analyzed at once. This makes comparisons of different specimens easier and reduces the analysis time. In the same paper photoluminescence spectra of two multi-layered paint specimens were compared using HSI [49]. Because both spectral and spatial data were gathered, differences in paint layers could easily be highlighted visually, as an alternative to a spectral comparison. This was also shown by Flynn et al who analyzed more multi-layered paint specimens using IR HSI [50]. They presented several ways to display hyperspectral data, which make chemical differences and similarities between heterogeneous specimens easy to visualize and understand for the layperson (such as a juror). The same applies to the visualization of differences in bicomponent fibers, as described in [51]. This study showed that infrared HSI can provide spatially resolved chemical information for those bicomponent fibers where it is possible to detect spectral differences between the two components present. As well as yielding

characteristic IR spectra of each component, the technique also provided images clearly illustrating the side-by-side configuration of these components in the fiber. However, in 5 of 11 bicomponent fibers no spectral differences were found using integrated peak intensities. Multivariate statistical analysis may improve these results. Markstrom and Mabbott also demonstrated the advantages of using HSI for the comparison of fibers [52] and addressed that the ability to compare fibers simultaneously in one measurement minimizes the chance for errors.

Miskelly and Wagner attempted to improve the visualization of chemically treated soil shoe marks using HSI [34]. The standard chemical enhancement technique for such marks is an acidic thiocyanate solution which reacts with iron (III) oxides in the soil to form a colored iron (III) thiocyanate complex. Unfortunately, this complex has a broad absorption band in the visible spectrum. They point at the necessity of enhancement chemicals with narrow absorption bands, as these can often be readily enhanced relative to the underlying background.

A forensic science application of remote sensing technology was demonstrated by Kalacska et al [53], who used airborne HSI for the detection of mass graves. Analysis of the spectra using Minimum Noise Fraction transform showed a clear separation between an experimental grave, a refilled empty grave, grass and forest. This indicates that airborne HSI can be used to detect the existence of suspicious decomposition properties, i.e. mass graves, which lead to differences in soil chemistry and vegetation.

Typical challenges

As demonstrated above, the application of HSI in forensic science casework brings specific challenges. In contrast to pure specimens usually analyzed in the laboratory, traces from casework can consist of complex contaminated mixtures. Next to this, the chemical composition of biological traces may change in time. Although these changes can be used for age estimation purposes [43,54], the influence of environmental conditions like temperature, humidity, precipitations and light should

be studied. For example the influence of temperature and humidity on the aging of blood stains is shown by Bremmer et al [55].

Also, traces are typically not found on ideal neutral reflecting backgrounds used in laboratories (see Figure 9). In casework, all possible backgrounds can be encountered (e.g. different materials, porous, non-porous, colored, patterned, etc.) which may complicate the measurements [27-31,35]. Comparison of spectra on different backgrounds typically requires advanced system calibration and data analysis. Miskelly and Wagner and Tahtouh et al examined the spectral properties of enhancement chemicals and experimented with new chemicals for the visualization of shoe marks [34] and fingerprints [36] respectively dedicated for the use of HSI. Although the use of chemicals is not preferred, this may help finding evidence.

The above mentioned challenges are not just characteristic for HSI, but are also valid for conventional spectroscopy. The transition from spectroscopy to HSI, however, is not straightforward. While specimen optical properties are independent of the spectral measurement system, the transition from spectroscopy to spectral imaging involves a drastic change in the illumination–collection geometry of the measurement system. Gebhardt et al showed that this change in measurement setup results in a disparity between measured spectra, which is dependent on the optical properties of the specimen and the optical path length [56]. Spectral data bases created for the identification of forensic traces like fibers or printer toners [57,58] may therefore need to be adapted to HSI applications.

Moving HSI from the laboratory to the scene of investigation brings further complications. Advances in wireless technology and sealed operating units are desirable to prevent contamination. Investigating scenes where chemical, biological, radiologic, or nuclear (CBRN) events have occurred poses dangers to investigators. In these cases, a remotely controlled robotic HSI system could provide important information instantly. However, these scenes have even more decontamination requirements.

The complex nature of crime scenes makes for challenging image analysis. Next to this, sunlight, external light sources, shadows and reflections from nearby objects all change the apparent illumination on an object. This variation can cause large variability in the measured spectra for a fixed object, a problem regularly encountered in remote sensing [59]. Algorithms are needed to distinguish this spectral variability due to non uniform illumination from spectral variability between objects.

Future applications

Despite the challenges, HSI offers great potential for providing new, valuable information in forensic science casework. HSI can be applied to detect traces by optimizing the contrast between a trace and its background, or to differentiate between traces, based on spectral differences. To create contrast between a trace and its background, crime scene investigators traditionally use commercially available light sources with different excitation and barrier filters to isolate regions of the spectrum where traces of interest have high absorption or photoluminescence. This way, e.g. semen and blood traces can be detected [60]. For laboratory purposes, dedicated forensic imaging systems are available with different light sources, excitation and barrier filters. These systems are mainly used in document analysis, e.g. for differentiating inks [61,62], but can also be applied in other fields, e.g. the visualization of gunshot residue patterns on dark clothing [63]. For all these purposes HSI can be used instead. Because HSI systems filter the light in many small bandwidths, maximum spectral differences can be calculated automatically and the choice of one specific filter is no longer necessary, which reduces the risk of human errors.

Many applications currently performed with conventional spectroscopy may also be enhanced with a spatial component using HSI, similar to the way presented for the identification [17,64,65], and age estimation of blood stains [18,54,65-68], as shown in Figure 9. In these applications, the added spatial information is crucial, as the blood stain pattern may reveal useful information for the reconstruction of a crime [69]. The spectroscopic identification of other body fluids [70] will also benefit from HSI, as the traces can then be interpreted in their original context.

The spatial distribution of components may be less important in fields like illicit drug analysis. However, using HSI instead of spectroscopic point measurements for the identification of drug components [71] may speed up the process, as many specimens can be imaged at once. The improved speed of HSI compared to spectroscopy, is particularly of advantage in hazardous environments. In explosives investigations especially, the ability to measure specimens without contact or specimen preparation is beneficial, as many accidents occur even when trained personnel handle explosives [72].

In 2000, Malkoff and Oliver proposed some interesting applications in forensic medicine which are not yet put into practice, like the analysis of patterned injuries (e.g. a tire print on the body of a victim), scanning of body and clothes for toxins, the aging of wounds through the spectral evaluation of local inflammation and repair, and the estimation of the time of death of a victim [73]. They also draw the attention to the need for crime scene reconstruction for operational planning, hazard identification, training etc. Crime scenes are often digitally captured using photography, and panoramic and 3D scanning techniques. These data can be used for a virtual crime scene reconstruction. The addition of HSI data to this reconstruction can give information about the chemical composition of traces and their distribution in the scene. Malkoff and Oliver claimed, this may help in body localization and retrieval, or the characterization of biological or chemical threats [73]. Using HSI, the chemical properties of the scene of investigation can be captured quickly without much disturbance to the scene and analysis can be performed afterwards in the original context.

Conclusion

Recent technological developments in HSI components have opened up the approach to forensic science applications. Fast acquisition, portable, high resolution systems are emerging facilitating the transfer of HSI from the laboratory to the field. Several forensic science applications of hyperspectral imaging were recently explored successfully. Challenges typically encountered in forensic science casework, e.g. contaminated traces found on non-ideal backgrounds in varying environmental

circumstances, emphasize the necessity to modify existing techniques and instrumentation. Key steps in the research process are refining and validating the data to meet the needs of the legal and scientific communities. When introduced in forensic science casework, hyperspectral imaging can help investigators detecting, visualizing and identifying useful traces non-destructively.

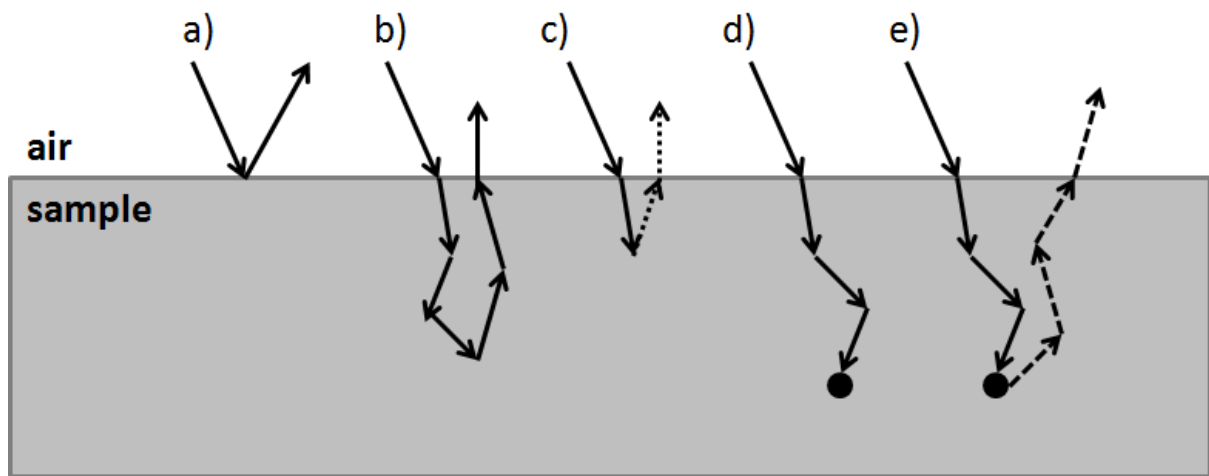


Figure 1. The interaction of light with a specimen may lead to a) specular reflection, b) elastic scattering followed by diffuse reflection, c) inelastic scattering followed by emission of Raman shifted light (dotted lines), d) absorption, and e) absorption followed by photoluminescence emission (dashed lines).

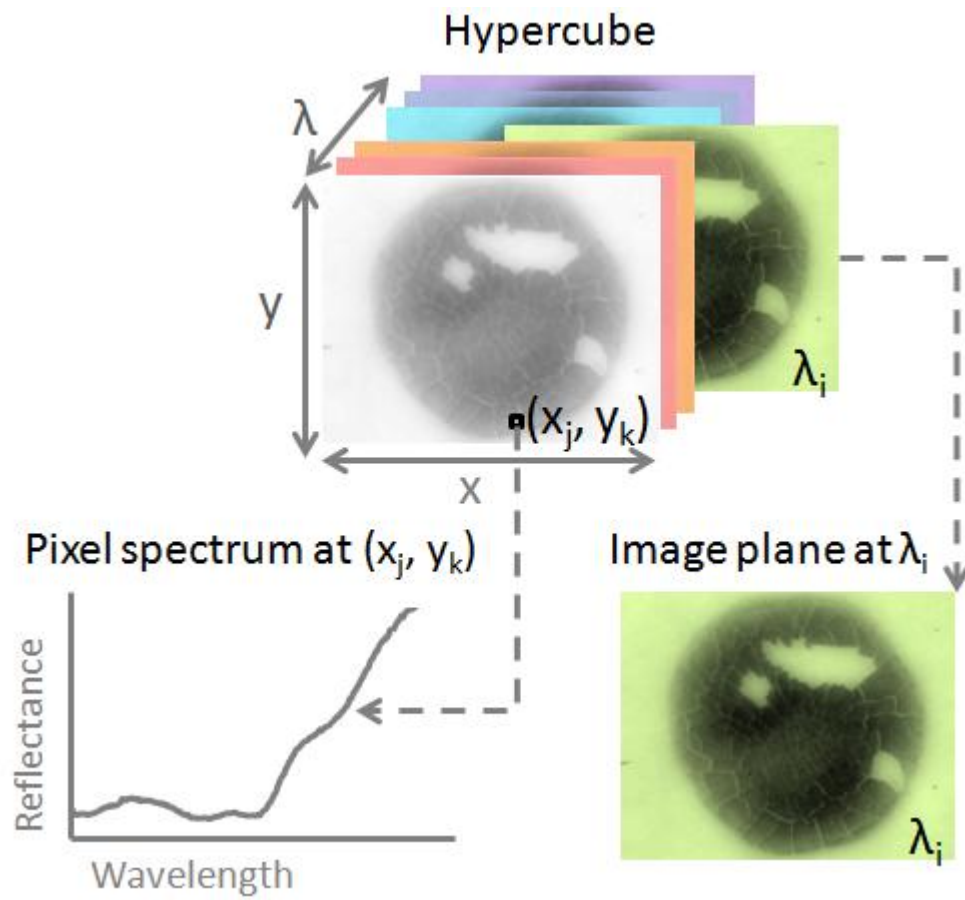


Figure 2. Hypercube of a blood stain, with two spatial (x,y) and one wavelength (λ) dimension. From the hypercube an image plane is shown for one wavelength (λ_i) and a spectrum is obtained from one pixel (x_j, y_k) .

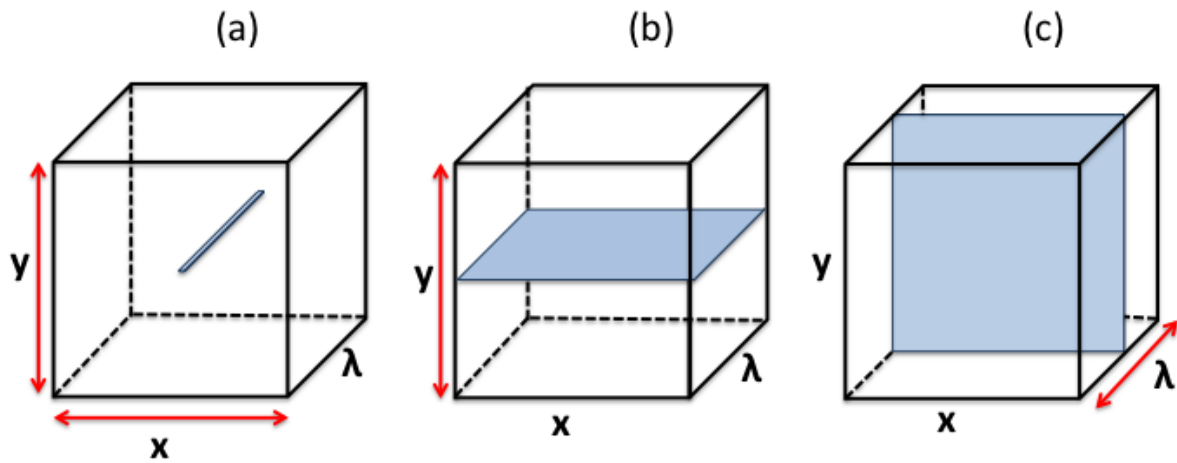


Figure 3. Methods for acquiring three-dimensional hypercubes: (a) point scanning, (b) line scanning, and (c) area scanning. Hypercubes contain two spatial (x, y) and one spectral (λ) dimension. Blue areas represent data acquired by one scan. Red arrows represent temporal scanning required to complete the hypercube.

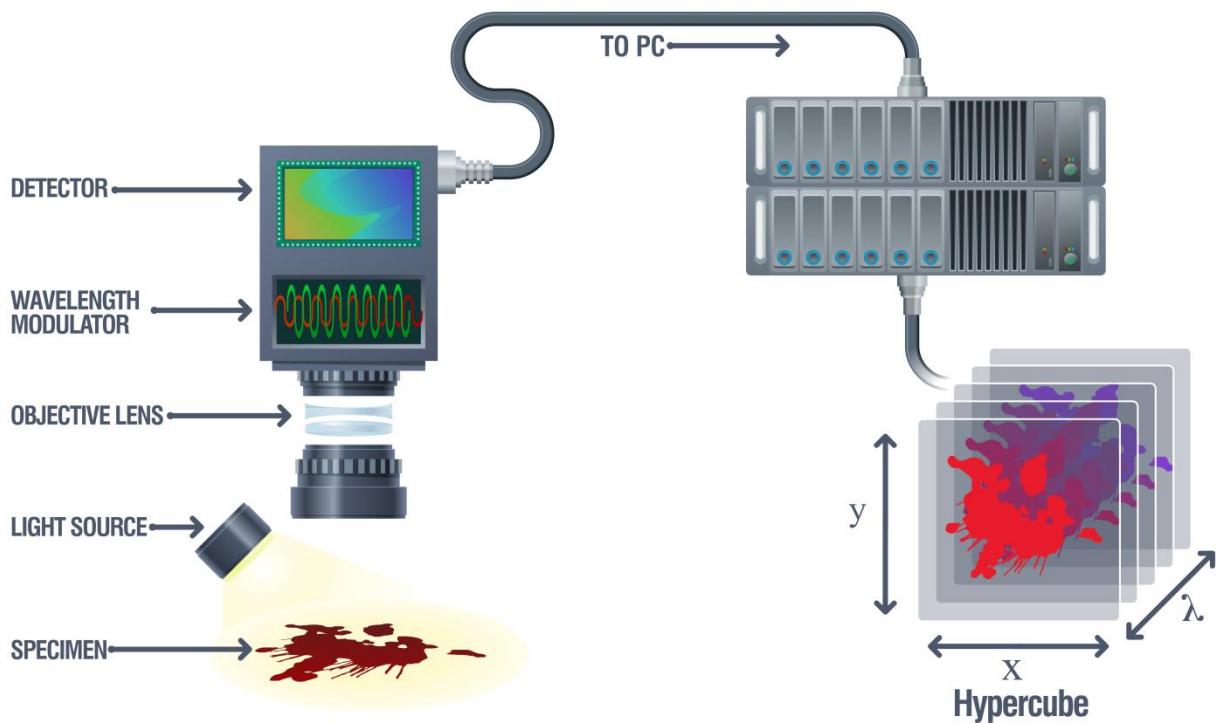


Figure 4. Schematic showing components of a HSI system, resulting in a hypercube of the specimen.



Figure 5. Hyperspectral imaging system at a simulated crime scene.

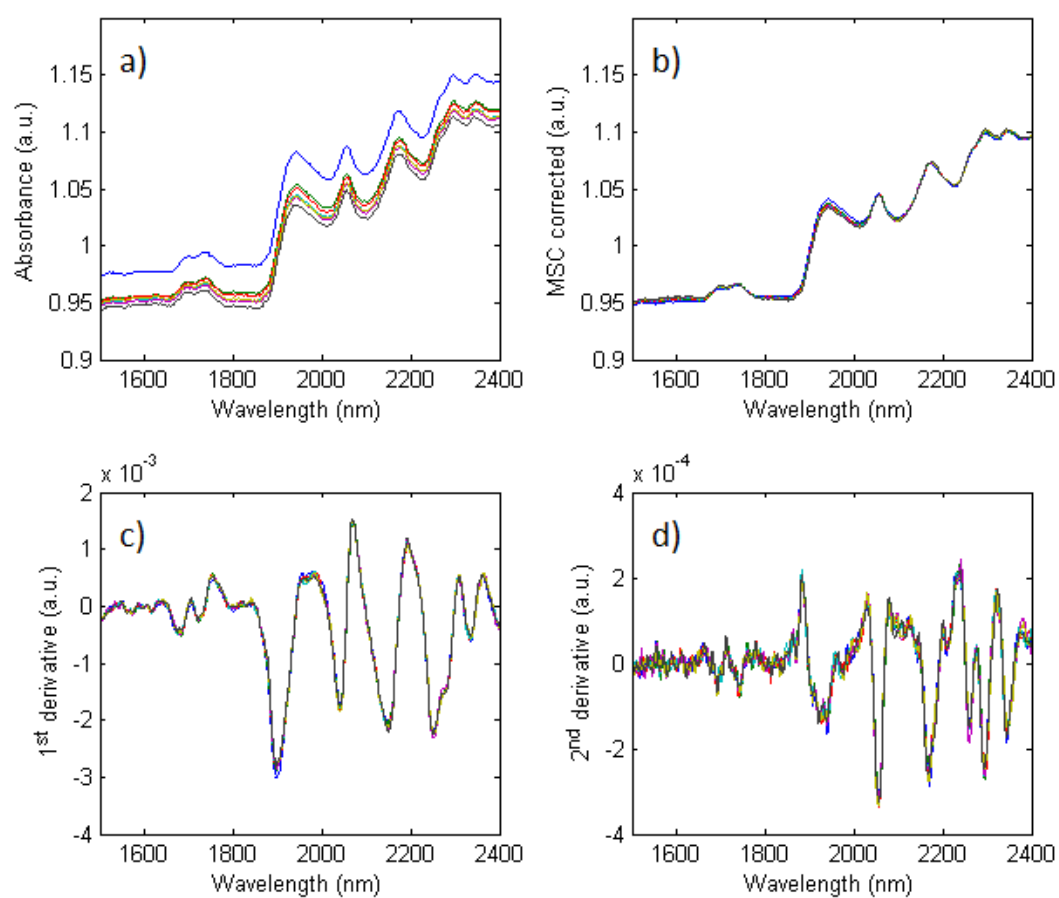


Figure 6. Spectra of several blood stains of the same age before and after pre-processing: a) absorbance spectra, b) spectra after applying multiplicative scatter correction (MSC), c) first derivative spectra, d) second derivative spectra.



Figure 7. Cut and flattened Dr. Pepper's soda can with fingermark deposit. (A) Soda can imaged by a document scanner. B) Infrared image of the outlined area obtained by plotting the band intensity at 9842 nm (1016 cm⁻¹). Reprinted from *Journal of Forensic Sciences*, 52/1, Nicole J. Crane, Edward G. Bartick, Rebecca Schwartz Perlman, Scott Huffman, *Infrared Spectroscopic Imaging for Noninvasive Detection of Latent Fingerprints*, 48-53, Copyright (2012), with permission from John Wiley and Sons [27].

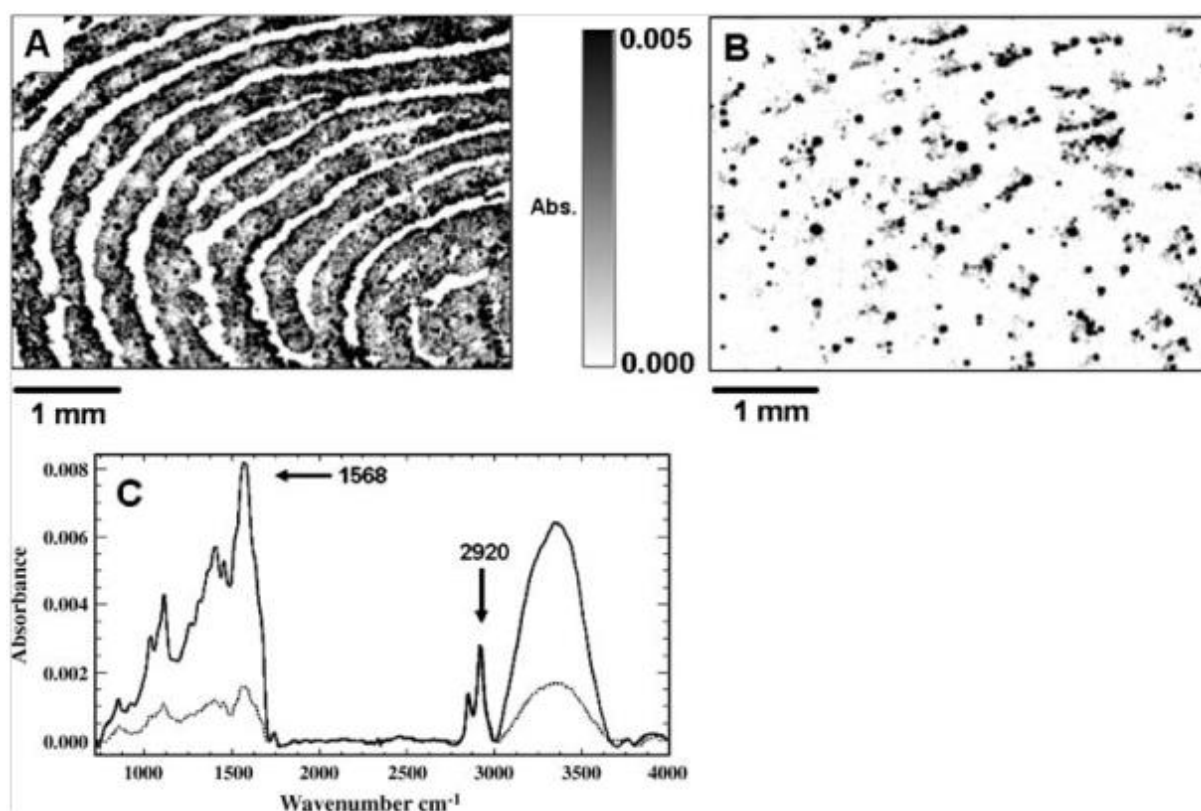


Figure 8. Images of a latent fingerprint developed by using different vibrational modes to highlight different aspects of the chemical composition of the deposited material. a) Print image developed by the absorbance magnitude at 2,920 cm^{-1} . and b) print image developed by absorbance magnitude at 1,568 cm^{-1} . c) Example spectra from the oil-rich region (top, dark line) and flake rich region are shown. Reprinted from *Analytical and Bioanalytical Chemistry*, 394/8, Rohit Bhargava, Non-invasive detection of superimposed latent fingerprints and inter-ridge trace evidence by infrared spectroscopic imaging, 2069–2075., Copyright (2012), with permission from Springer.

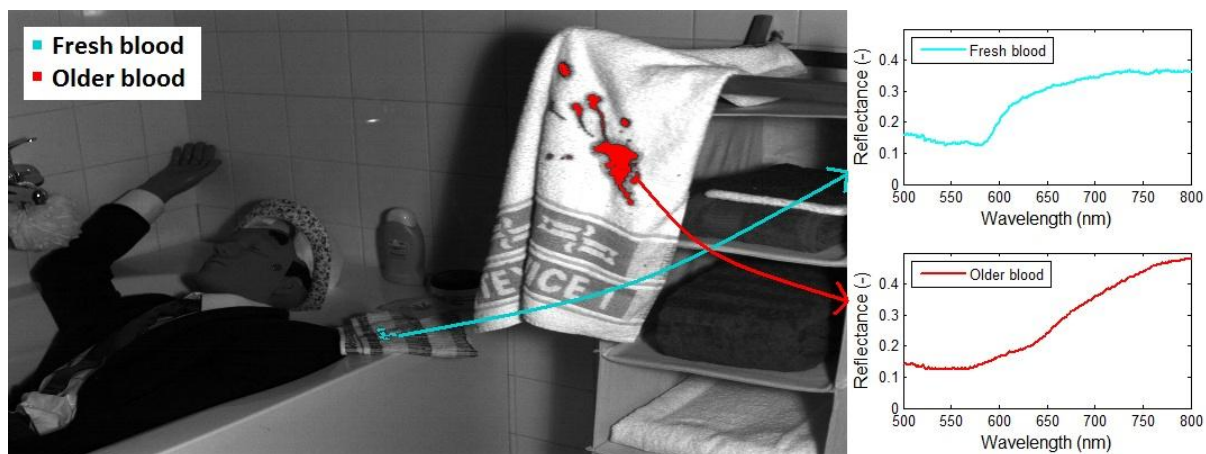


Figure 9. Simulated crime scene, in which fresh and older blood stains were automatically detected and distinguished (left) based on their reflectance spectra (right).



Figure 10. Third principal component of blue ink set, indistinguishable with the human eye.

Reprinted from Talanta, 67/2, Gemma Payne et al, Visible and near-infrared chemical imaging

methods for the analysis of selected forensic specimens, 334–344 Copyright (2012), with permission from Elsevier [50].

References

1. M. Govender, K. Chetty, H. Bulcock, A review of hyperspectral remote sensing and its application in vegetation and water resource studies, *Water Sa.* 33 (2007) 145-151.
2. A.A. Gowen, C.P. O'Donnell, P.J. Cullen, G. Downey, J.M. Frias, Hyperspectral imaging - an emerging process analytical tool for food quality and safety control, *Trends Food Sci. Technol.* 18 (2007) 590-598.
3. A.A. Gowen, C.P. O'Donnell, P.J. Cullen, S.E. Bell, Recent applications of Chemical Imaging to pharmaceutical process monitoring and quality control, *Eur. J. Pharm. Biopharm.* 69 (2008) 10-22.
4. Levenson, R.M., E.S. Wachman, W. Niu, D.L. Farkas, Spectral imaging in biomedicine: a selective overview, *Proceedings of SPIE, Imaging Spectrometry IV*, 3438 (1998), 300-312.
5. R.H. Bremmer, S.C. Kanick, N. Laan, A. Amelink, T.G. van Leeuwen, M.C. Aalders, Non-contact spectroscopic determination of large blood volume fractions in turbid media, *Biomed. Opt. Express.* 2 (2011) 396-407.
6. Suhre, D.R., L.H. Taylor, N.B. Singh, W.R. Rosch, Comparison of acousto-optic tunable filters and acousto-optic dispersive filters for hyperspectral imaging, *Proceedings of SPIE, 27th AIPR Workshop: Advances in Computer-Assisted Recognition*, 3584 (1999), 142-147.
7. M.D. Evans, C.N. Thai, J.C. Grant, Development of a spectral imaging system based on a liquid crystal tunable filter, *Transactions of the ASAE.* 41 (1998) 1845-1852.
8. E. Margalith, R.J. Barnes, Spectral imaging device with tunable light source. I. Opotek, 19-6-2007, US7233392.
9. Qin, J., *Instruments for Constructing Hyperspectral Imaging Systems (Eds.)*, *Hyperspectral Imaging for Food Quality Analysis and Control*, Elsevier, New York, 2010, pp. 133-172.
10. Kirkhus, T., B.G. Fismen, J. Tschudi, M. O'Farrell, Calibration of a Multi-Object Spectrometer with Programmable and Arbitrary Field of View, *Spectroscopy, Color, & Imaging II, Applied Industrial Optics: Spectroscopy, Imaging and Metrology*, (2010),
11. H.F. Grahn, P. Geladi, *Techniques and Applications of Hyperspectral Image Analysis*, John Wiley & Sons, Ltd, Chichester, 2007.
12. P. Geladi, J. Burger, T. Lestander, Hyperspectral imaging: calibration problems and solutions, *Chemometrics and Intelligent Laboratory Systems.* 72 (2004) 209-217.
13. R.J. Barnes, M.S. Dhanoa, S.J. Lister, Standard Normal Variate Transformation and De-trending of Near-Infrared Diffuse Reflectance Spectra, *Appl. Spectrosc.* 43 (1989) 772-777.
14. J. Burger, PhD thesis: Hyperspectral NIR image analysis: data exploration, correction and regression.(2006).
15. A. Savitzky, M.J.E. Golay, Smoothing and Differentiation of Data by Simplified Least Squares Procedures, *Anal. Chem.* (1964) 1627-1639.

16. F. van der Meer, The effectiveness of spectral similarity measures for the analysis of hyperspectral imagery, *International Journal of Applied Earth Observation and Geoinformation*. 8 (2006) 3-17.
17. G.J. Edelman, T.G. van Leeuwen, M.C.G. Aalders, Hyperspectral imaging of the crime scene for the automatic detection and identification of blood stains, *Forensic Sci. Int.* Submitted (2012) .
18. G.J. Edelman, T.G. van Leeuwen, M.C.G. Aalders, Hyperspectral imaging for the age estimation of blood stains at the crime scene, *Forensic Sci. Int.* In press (2012) .
19. N. Keshava, J.F. Mustard, Spectral unmixing, *Ieee Signal Processing Magazine*. 19 (2002) 44-57.
20. Alam, M.S., M.I. Elbakary, M.S. Aslan, Object detection in hyperspectral imagery by using K-means clustering algorithm with pre-processing, *Proceedings of SPIE, Optical Pattern Recognition XVIII*, (2007),
21. S. Wold, M. Sjostrom, L. Eriksson, PLS-regression: a basic tool of chemometrics, *Chemometrics and Intelligent Laboratory Systems*. 58 (2001) 109-130.
22. H.Z.M. Shafri, A. Suhaili, S. Mansor, The Performance of Maximum Likelihood, Spectral Angle Mapper, Neural Network and Decision Tree Classifiers in Hyperspectral Image Analysis, *J. Comp. Sci.* 3 (2007) 419-423.
23. B.K. Alsberg, T. Loke, I. Baarstad, PryJector: A Device for In Situ Visualization of Chemical and Physical Property Distributions on Surfaces Using Projection and Hyperspectral Imaging, *J. Forensic Sci.* 56 (2011) 976-983.
24. P.H. Ng, S. Walker, M. Tahtouh, B. Reedy, Detection of illicit substances in fingerprints by infrared spectral imaging, *Anal. Bioanal. Chem.* 394 (2009) 2039-2048.
25. Ramotowski, R., *Composition of Latent Print Residue (Eds.)*, *Advances in Fingerprint Technology*, CRC Press, Boca Raton, FL, 2001, pp. 63-104.
26. Bartick, E., R. Schwartz, R. Bhargava, M. Schaeberle, D. Fernandez, I. Levin, Spectrochemical analysis and hyperspectral imaging of latent fingerprints, 16th Meeting of the International Association of Forensic Sciences, (2002),
27. N.J. Crane, E.G. Bartick, R.S. Perlman, S. Huffman, Infrared spectroscopic imaging for noninvasive detection of latent fingerprints, *J. Forensic Sci.* 52 (2007) 48-53.
28. D.L. Exline, C. Wallace, C. Roux, C. Lennard, M.P. Nelson, P.J. Treado, Forensic applications of chemical imaging: latent fingerprint detection using visible absorption and luminescence, *J. Forensic Sci.* 48 (2003) 1047-1053.
29. G. Payne, B. Reedy, C. Lennard, B. Comber, D. Exline, C. Roux, A further study to investigate the detection and enhancement of latent fingerprints using visible absorption and luminescence chemical imaging, *Forensic Sci. Int.* 150 (2005) 33-51.
30. M. Tahtouh, J.R. Kalman, C. Roux, C. Lennard, B.J. Reedy, The detection and enhancement of latent fingermarks using infrared chemical imaging, *J. Forensic Sci.* 50 (2005) 64-72.

31. M. Tahtouh, P. Despland, R. Shimmon, J.R. Kalman, B.J. Reedy, The application of infrared chemical imaging to the detection and enhancement of latent fingerprints: method optimization and further findings, *J. Forensic Sci.* 52 (2007) 1089-1096.
32. R. Bhargava, R.S. Perlman, D.C. Fernandez, I.W. Levin, E.G. Bartick, Non-invasive detection of superimposed latent fingerprints and inter-ridge trace evidence by infrared spectroscopic imaging, *Anal. Bioanal. Chem.* 394 (2009) 2069-2075.
33. C. Champod, C. Lennard, P. Margot, M. Stoilovic, *Fingerprints and Other Ridge Skin Impressions*, CRC Press, 2004.
34. G.M. Miskelly, J.H. Wagner, Using spectral information in forensic imaging, *Forensic Sci. Int.* 155 (2005) 112-118.
35. P. Maynard, J. Jenkins, C. Edey, G. Payne, C. Lennard, A. McDonagh, C. Roux, Near infrared imaging for the improved detection of fingermarks on difficult surfaces, *Aust. J. Forensic Sci.* 41 (2009) 43-62.
36. M. Tahtouh, S.A. Scott, J.R. Kalman, B.J. Reedy, Four novel alkyl 2-cyanoacrylate monomers and their use in latent fingermark detection by mid-infrared spectral imaging, *Forensic Sci. Int.* 207 (2011) 223-238.
37. A. Grant, T.J. Wilkinson, D.R. Holman, M.C. Martin, Identification of recently handled materials by analysis of latent human fingerprints using infrared spectromicroscopy, *Appl. Spectrosc.* 59 (2005) 1182-1187.
38. E.D. Emmons, A. Tripathi, J.A. Guicheteau, S.D. Christesen, A.W. Fountain, III, Raman chemical imaging of explosive-contaminated fingerprints, *Appl. Spectrosc.* 63 (2009) 1197-1203.
39. T. Chen, Z.D. Schultz, I.W. Levin, Infrared spectroscopic imaging of latent fingerprints and associated forensic evidence, *Analyst.* 134 (2009) 1902-1904.
40. K.S. Kalasinsky, J. Magluilo, Jr., T. Schaefer, Hair analysis by infrared microscopy for drugs of abuse, *Forensic Sci. Int.* 63 (1993) 253-260.
41. K.S. Kalasinsky, Drug distribution in human hair by infrared microscopy, *Cell Mol. Biol. (Noisy-le-grand)*. 44 (1998) 81-87.
42. C. Birngruber, F. Ramsthaler, M.A. Verhoff, The color(s) of human hair--forensic hair analysis with SpectraCube, *Forensic Sci. Int.* 185 (2009) e19-e23.
43. P. Tramini, B. Bonnet, R. Sabatier, L. Maury, A method of age estimation using Raman microspectrometry imaging of the human dentin, *Forensic Sci. Int.* 118 (2001) 1-9.
44. Randeberg, L. L., Skallerud, B., Langlois, N., Haugen, O. A., and Svaasand, L. O., *The Optics of Bruising (Eds.), Optical-Thermal Response of Laser-Irradiated Tissue*, Springer Science+Business Media B.V., 2011, pp. 825-858.
45. G. Payne, N. Langlois, C. Lennard, C. Roux, Applying visible hyperspectral (chemical) imaging to estimate the age of bruises, *Med. Sci. Law.* 47 (2007) 225-232.

46. L.L. Randeberg, E.L. Larsen, L.O. Svaasand, Characterization of vascular structures and skin bruises using hyperspectral imaging, image analysis and diffusion theory, *J. Biophotonics*. 3 (2010) 53-65.
47. B. Stam, M.J.C. van Gemert, T.G. van Leeuwen, A.H. Teeuw, A.C. van der Wal, M.C.G. Aalders, Can color inhomogeneity of bruises be used to establish their age?, *J. Biophotonics*. 4 (2011) 759-767.
48. J. Wolfe, D.L. Exline, Characterization of condom lubricant components using Raman spectroscopy and Raman chemical imaging, *J. Forensic Sci.* 48 (2003) 1065-1074.
49. G. Payne, C. Wallace, B. Reedy, C. Lennard, R. Schuler, D. Exline, C. Roux, Visible and near-infrared chemical imaging methods for the analysis of selected forensic specimens, *Talanta*. 67 (2005) 334-344.
50. K. Flynn, R. O'Leary, C. Lennard, C. Roux, B.J. Reedy, Forensic applications of infrared chemical imaging: multi-layered paint chips, *J. Forensic Sci.* 50 (2005) 832-841.
51. K. Flynn, R. O'Leary, C. Roux, B.J. Reedy, Forensic analysis of bicomponent fibers using infrared chemical imaging, *J. Forensic Sci.* 51 (2006) 586-596.
52. L.J. Markstrom, G.A. Mabbott, Obtaining absorption spectra from single textile fibers using a liquid crystal tubable filter microspectrophotometer, *Forensic Sci. Int.* 209 (2011) 108-112.
53. M.E. Kalacska, L.S. Bell, G. Sanchez-Azofeifa, T. Caelli, The Application of Remote Sensing for Detecting Mass Graves: An Experimental Animal Case Study from Costa Rica, *J. Forensic Sci.* 54 (2009) 159-166.
54. R.H. Bremmer, A. Nadort, T.G. van Leeuwen, M.J. van Gemert, M.C. Aalders, Age estimation of blood stains by hemoglobin derivative determination using reflectance spectroscopy, *Forensic Sci. Int.* 206 (2011) 166-171.
55. R.H. Bremmer, D.M. de Bruin, M. de Joode, W.J. Buma, T.G. van Leeuwen, M.C.G. Aalders, Biphasic Oxidation of oxy-hemoglobin in bloodstains, *PLoS One*. (2011) .
56. S.C. Gebhart, S.K. Majumder, A. Mahadevan-Jansen, Comparison of spectral variation from spectroscopy to spectral imaging, *Appl. Optics*. 46 (2007) 1343-1360.
57. M.W. Tungol, E.G. Bartick, A. Montaser, Spectral Data-Base for the Identification of Fibers by Infrared Microscopy, *Spectrochimica Acta Part B-Atomic Spectroscopy*. 46 (1991) e1535-e1544.
58. R.A. Merrill, E.G. Bartick, J.H. Taylor, Forensic discrimination of photocopy and printer toners. I. The development of an infrared spectral library, *Anal. Bioanal. Chem.* 376 (2003) 1272-1278.
59. Adler-Golden, S.M., R.Y. Levine, M.W. Matthew, S.C. Richtsmeier, L.S. Bernstein, J. Gruninger, G. Felde, M. Holke, G. Anderson, A. Ratkowski, Shadow-insensitive material detection/classification with atmospherically corrected hyperspectral imagery , *SPIE*, (2001),
60. M. Stoilovic, Detection of Semen and Blood Stains Using Polilight As A Light-Source, *Forensic Sci.Int.* 51 (1991) 289-296.

61. M. Kunicki, Differentiating blue ballpoint pen inks, *Prob. Forensic. Sci. LI.* (2002) 56-70.
62. G.M. Mokrzycki, *Advances in Document Examination: The Video Spectral Comparator 2000*, *Forensic Sci.Comm.* 1 (1999) .
63. C.S. Atwater, M.E. Durina, J.P. Durina, R.D. Blackledge, Visualization of gunshot residue patterns on dark clothing, *J. Forensic Sci.* 51 (2006) 1091-1095.
64. R.H. Bremmer, G. Edelman, T.D. Vegter, T. Bijvoets, M.C.G. Aalders, Remote Spectroscopic Identification of Bloodstains, *J. Forensic Sci.* 56 (2011) 1471-1475.
65. G.J. Edelman, V. Manti, S.M. van Ruth, T.G. van Leeuwen, M.C.G. Aalders, Identification and age estimation of blood stains on colored backgrounds by near infrared spectroscopy, *Forensic Sci. Int.* 220 (2012) 239-244.
66. E. Botonjic-Sehic, C.W. Brown, M. Lamontagne, M. Tsaparikos, Forensic Application of Near-Infrared Spectroscopy: Aging of Bloodstains, *Spectroscopy.* 24 (2009) 42-49.
67. Y.L. Liu, R.K. Cho, K. Sakurai, T. Miura, Y. Ozaki, Studies on Spectra-Structure Correlations in Near-Infrared Spectra of Proteins and Polypeptides .1. A Marker Band for Hydrogen-Bonds, *Appl. Spectroscopy.* 48 (1994) 1249-1254.
68. B. Li, P. Beveridge, W.T. O'Hare, M. Islam, The estimation of the age of a blood stain using reflectance spectroscopy with a microspectrophotometer, spectral pre-processing and linear discriminant analysis, *Forensic Sci. Int.* in press (2011) .
69. O. Peschel, E. Muetzel, M.A. Rothschild, Blood stain pattern analysis, *Rechtsmedizin.* 18 (2008) 131-145.
70. K. Virkler, I.K. Lednev, Forensic body fluid identification: The Raman spectroscopic signature of saliva, *Analyst.* 135 (2010) 512-517.
71. C.M. Hodges, J. Akhavan, The Use of Fourier-Transform Raman-Spectroscopy in the Forensic Identification of Illicit Drugs and Explosives, *Spectrochimica Acta Part A-Molecular and Biomolecular Spectroscopy.* 46 (1990) 303-307.
72. McNesby, K. L. and Pesce-Rodriguez, R. A., Applications of vibrational spectroscopy in the study of explosives (Eds.), *Handbook of Vibrational Spectroscopy.*, John Wiley & Sons Ltd., Chichester, England, 2002, pp. 3152-3168.
73. Malkoff, D.B., W.R. Oliver, Hyperspectral imaging applied to forensic medicine, *SPIE, Spectral imaging: Instrumentation, Applications and Analysis*, 3920 (2000), 108-116.

Table 1. List of applications reviewed in this paper. For each application, the measurement mode, wavelength range, wave number range and reference is given. Wavelength and wave number ranges are copied or converted from information available in the references.

Application	Mode	Wavelength range (nm)	Wave number range (cm ⁻¹)	Reference
Untreated fingerprints	Reflectance	2500-11111	900-4000	[26]
	Reflectance	2500-14285	700-4000	[27]
	Reflectance	400-720	13888-25000	[28]
	Reflectance	400-720	13888-25000	[29]
	Reflectance	2500-11111	900-4000	[30]
	Reflectance	2500-11111	900-4000	[31]
	Reflectance	2500-11111	900-4000	[32]
Treated fingerprints	Reflectance,	400-720	13888-25000	[28]
	Luminescence			
	Reflectance,	400-720	13888-25000	[29]
	Luminescence			
	Reflectance	2500-11111	900-4000	[30]
	Reflectance	2500-11111	900-4000	[31]
	Reflectance,	400-700	14285-25000	[34]
	Luminescence			
	Reflectance,	650 – 1100	9090-15384	[35]
	Luminescence			
	Reflectance	2500-11111	900-4000	[36]
Traces in fingerprints	Reflectance	2500-11111	900-4000	[37]
	Reflectance	2500-11111	900-4000	[32]
	Reflectance,	2500-11111	900-4000	[24]
	Transmission			
	Raman,	546-590	16950-18300,	[38]
	Photoluminescence	400-720	13888-25000	
	Reflectance	2500-14285	700-4000	[39]
Drugs in hair	Reflectance	2500-11111	900-4000	[40]

	Reflectance	2500-11111	900-4000	[41]
Hair	Transmission	450-1000	10000-22222	[42]
Dentin	Raman	645-800	12522-15472	[43]
Bruises	Reflectance	410-550	18181-24390	[45]
	Reflectance	400-1000	10000-25000	[46]
	Reflectance	440-700	14285-22727	[47]
Blood stains	Reflectance	500-800	12500-20000	[17]
	Reflectance	500-800	12500-20000	[18]
Condoms	Raman	625-640	15650-16000	[48]
Inks	Reflectance, Photoluminescence	400-720	13888-25000	[49]
Tapes	Photoluminescence	400-720	13888-25000	[49]
Firearm propellants	Reflectance, Photoluminescence	400-720	13888-25000	[49]
Paints	Reflectance, Photoluminescence	400-720	13888-25000	[49]
	Transmission	2500-11111	900-4000	[50]
Fibers	Transmission	2500-11111	900-4000	[51]
	Reflectance	400-720	13888-25000	[52]

- (1) Margalith, E.; Office, U. P., Ed. 2007.
- (2) Tahtouh, M.; Despland, P.; Shimmon, R.; Kalman, J. R.; Reedy, B. J. *Journal of Forensic Sciences* **2007**, 52, 1089.
- (3) Tahtouh, M.; Kalman, J. R.; Roux, C.; Lennard, C.; Reedy, B. J. *Journal of Forensic Sciences* **2005**, 50, 64.
- (4) Kalasinsky, K. S.; Maguilolo Jr, J.; Shcafer, T. *Forensic Science International* **1993**, 63, 253.